Journal of Applied Mechanics and Technical Physics, Vol. 50, No. 1, pp. 127–136, 2009

THEORETICAL AND EXPERIMENTAL STUDY OF ENERGY DISSIPATION IN THE COURSE OF STRAIN LOCALIZATION IN IRON

O. A. Plekhov and O. B. Naimark

UDC 539.3, 621.384.3

Plastic strain localization is studied with the use of a high-sensitivity infrared camera. Plastic strain localization in iron is demonstrated to be accompanied by the emergence of heat waves and their propagation over the sample surface. Constitutive equations that describe the energy balance in the material under plastic strains are derived, and the plastic flow of iron is analyzed. The results of research are compared with the data obtained by infrared scanning. The proposed model of strain localization in the form of soliton-like waves (phase triggering waves) is demonstrated to agree with the kinetics of temperature waves characterizing dissipation inherent in the development of plastic deformation.

Key words: *thermodynamics and mesomechanics of defects, energy dissipation, infrared thermography.*

INTRODUCTION

The results of studying the evolution of the structure of metallic materials under plastic strain, which have been performed for the last decades, show that the most important feature of the plastic flow is plastic strain localization. The major part of publications deal with studying the mechanics of this process accompanied by changes in system properties because its behavior becomes controlled by the dynamics of regions with localized shear [1].

The interest in this problem has recently increased because it became possible to check the theoretical models experimentally. Infrared scanning for studying the balance and redistribution in the material of energy spent on deformation of a representative volume of the sample offers more detailed knowledge on the mechanisms of plastic strain localization.

The relationship between plastic strain and kinetics of phase triggering waves caused by dissipative effects in strain localization region was established in [2] by an example of the S355MC steel. It was shown that the velocity of propagation of heat waves depends on the strain rate, and their amplitude can reach 3–4°. The mechanisms of propagation of strain localization waves in single-crystal metals with an face-centered cubic lattice (copper and nickel) were studied in [3]. Kiselev [4] proposed a mathematical model of propagation of localized plasticity waves in crystals, based on the mechanism of double cross-slips of the screw-dislocation segments.

In the development of physical models that describe the specific features of dissipative processes caused by collective properties of ensembles of mesodefects and their influence on the nature of structural relaxation, some of the assumptions on plastic strain mechanisms based on the ideas of [5] were reconsidered.

Institute of Mechanics of Continuous Media, Ural Division, Russian Academy of Sciences, Perm' 614013; poa@icmm.ru; naimark@icmm.ru. Translated from Prikladnaya Mekhanika i Tekhnicheskaya Fizika, Vol. 50, No. 1, pp. 153–164, January–February, 2009. Original article submitted April 10, 2007; revision submitted December 17, 2007.

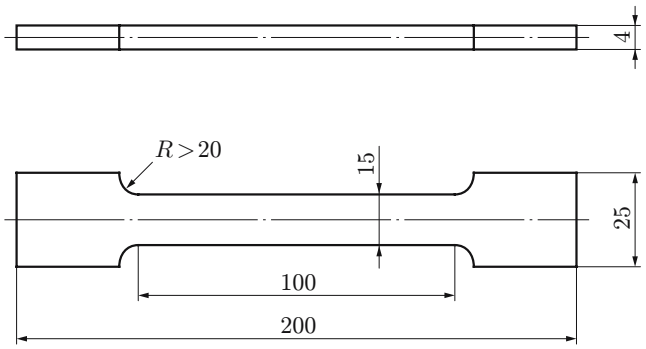

Fig. 1. Shapes and geometric sizes of the samples.

The use of the approach [6, 7] to the description of the behavior of media with mesodefects, based on generalization of methods of statistical thermodynamics for nonequilibrium systems, allowed for establishing a relationship between the mechanisms of structural relaxation with nonlinear laws of plastic deformation and transitions from damage to strain localization and failure.

The phenomenology of this approach is based on the formulation of the nonequilibrium mesoscopic potential: nonequilibrium free energy, which takes into account the nonlinearity types typical of materials with mesodefects. The form of the mesoscopic potential is based on the statistical description of the behavior of an ensemble of mesodefects. It is a generalization of the Ginzburg–Landau potential for an established new class of critical phenomena: structural scaling transitions typical of solid-state nonequilibrium systems with mesodefects. A specific feature of this potential is its dependence on an additional order parameter: parameter of structural scaling, which takes into account multiscale interactions in the ensemble of mesodefects. The use of the notions of the structural scaling transitions in studying a wide class of mesoscopic systems with defects allowed an analysis of wave effects and dissipative mechanisms accompanying the processes of structural relaxation and localization of plastic flow [7].

An important problem in model verification is determining the constants that characterize the kinetics of mesodefect development and effects of nonlocality, which have to be taken into account in describing the behavior of mesodefect ensembles. In the present work, we demonstrate that infrared scanning of wave processes caused by strain localization allows verification of the theoretical model that describes the energy balance in a material under plastic strain and estimation of the material parameters of the model.

1. EXPERIMENTAL STUDY OF DISSIPATION WAVES IN IRON

1.1. Test Conditions. The experiment was carried out on thermally treated samples of armco-iron under conditions of isothermal deformation. The samples had the following chemical composition: 0.004% C, 0.04% Mn, 0.05% Si, 0.005% S, 0.005% P, 0.06% Ni, 0.038% Cr, 0.01% Mo, and more than 99% Fe.

The geometry of the samples is shown in Fig. 1. After mechanical treatment, the samples were subjected to annealing in an oxygen-free atmosphere at a temperature of 800°C during 8 h. For monitoring of energy dissipation, the sample surface was mechanically polished in several stages (at the last stage, a diamond suspension with inclusions with a typical size of 3 μm was used) and was coated by a mat black paint. The samples were loaded in the regime of uniaxial tension with a strain rate $\dot{\varepsilon} = 10^{-4}$–$2 \cdot 10^{-3}$ sec^{-1}.

The evolution of the temperature field was recorded by a CEDIP Jade III infrared camera. The spectral range of the camera is 3–5 μm. The maximum frame size is 320×240 pixels, the minimum spatial size of the "heat" point is 10^{-4} m, the minimum error of temperature measurement is 25 mK for a sample temperature of 300 K, and the maximum frame rate is 500 Hz. The surface was studied by a New View 5000 optical interferometer-profilometer, which allows obtaining a three-dimensional image of the relief with a horizontal resolution within 0.5 μm and vertical resolution within 1 nm.

1.2. Experimental Results. The experimental technique and test results are described below.

Algorithm of Calculating the Sizes and Locations of Heat Sources. The locations of heat sources were calculated by an algorithm similar to that proposed in [8]. The coordinate system was chosen so that the tension

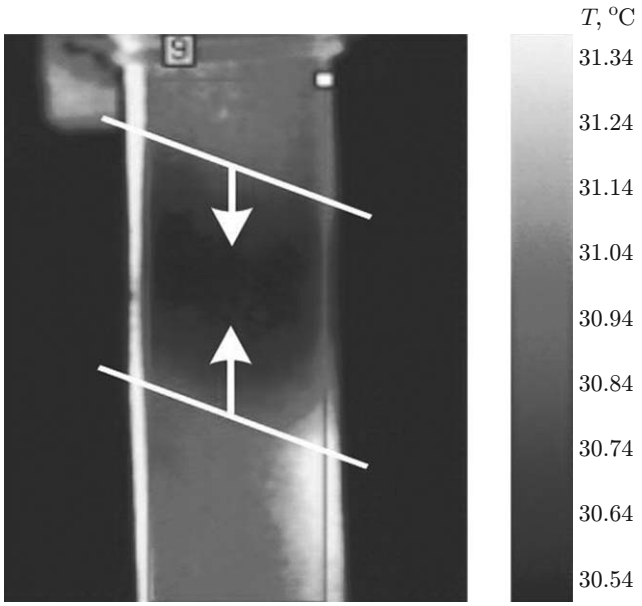

Fig. 2. Temperature distribution on the sample surface for a strain rate $\dot{\varepsilon} = 2 \cdot 10^{-3}$ sec^{-1} (the arrows indicate the directions of motion of strain waves).

direction coincided with the x axis, and the y axis was located in the plane of the sample. The temperature field across the sample (in the z direction) was assumed to be uniform.

The equation that determines the power of heat sources follows from the heat-conduction equation

$$r(x, y, t) = \rho c\dot{T}(x, y, t) - k\Delta T(x, y, t),$$

where ρ is the density, k is the thermal conductivity, and c is the heat capacity.

The results of infrared scanning in cross sections $y = \text{const}$ were processed by means of the discrete Fourier transform (DFT) to reduce the effect of random oscillations of temperature. A mirror reflection of the signal with respect to the y axis was used in DFT calculations. The direct and inverse DFTs can be presented as

$$T\omega_k = \sum_{n=0}^{N-1} T_n \exp\Big(2\pi ni\,\frac{k}{N}\Big), \qquad T_n = \frac{1}{N}\sum_{k=0}^{N-1} T\omega_k \exp\Big(-2\pi ni\,\frac{k}{N}\Big) \qquad (k, n = 0, 1, \ldots, N-1)$$

or

$$T\omega_k = F(T_n), \qquad T_n = F^{-1}(T\omega_k).$$

The function $\varphi(x) = (\nu_c/\sqrt{\pi}\,)\exp(-\nu_c^2 x^2)$ was used as a filter.

The power of heat sources was determined as follows:

$$T_f(t) = \mathrm{Re}\,[NF^{-1}(F(T)F(\varphi))], \qquad \Delta T_f(t) = \mathrm{Re}\,[NF^{-1}(F(T)F(\Delta\varphi))],$$

$$r(x, t) = \rho c\dot{T}_f(x, t) + k\Delta T_f(x, t).$$

Here $T_f(t)$ and $\Delta T_f(t)$ are the filtered values of $T(t)$ and $\Delta T(t)$; $\Delta\varphi = (4\nu_c^5/\sqrt{\pi}\,)\exp(-\nu_c^2 x^2)(r^2 - 1/(2\nu_c^2))$.

Calculated Distributions of Heat Sources. The calculated results are plotted in Figs. 2–4. Figure 2 shows the spatial distribution of temperature on the sample surface for a strain rate $\dot{\varepsilon} = 0.002$ sec^{-1}. Two localized strain waves move from the clutches toward the sample surface at an angle of 70° (the length of the examined region is 48.85 mm, and the time needed for the waves to pass is 21.5 sec). Figure 3a shows the corresponding space–time evolution of temperature in the sample cross section. An analysis of the temperature-field kinetics allows us to reconstruct the space–time distribution of heat sources in the sample (Fig. 3b). The zone with intense dissipation of energy is approximately 15–20 mm wide. When the waves meet, the dissipation activity in the sample is substantially enhanced.

Figure 4 shows the local strain in the sample as a function of time. The data were obtained from an external mechanical extensometer. Outside the localized strain wave, the strain rate equals zero until the wave fronts meet.

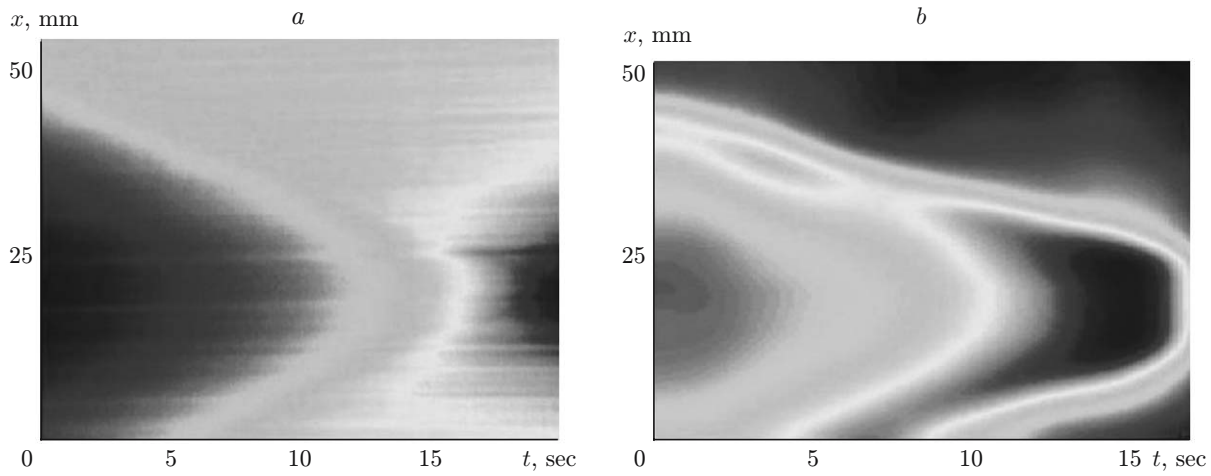

Fig. 3. Space–time evolution of the temperature field (a) and the corresponding distribution of heat sources (b) obtained in experiments.

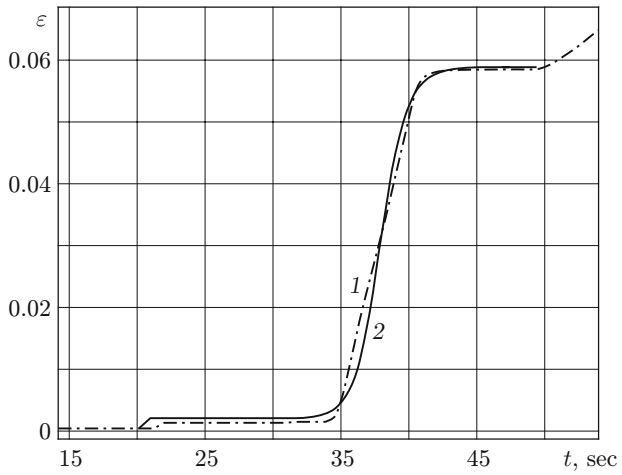

Fig. 4. Local strain in the sample versus time at the moment of the transition of the strain wave: curves 1 and 2 show the experimental data and the numerical calculations, respectively.

2. PROPERTIES OF MESODEFECTS

2.1. Order Parameters for Media with Defects. Determining the independent variables characterizing plastic strain is an urgent problem. It was noted [9] that plastic strain is the result of motion of dislocation-type defects; therefore, it is necessary to introduce structural variables determining the thermodynamic state of a plastically strained solid. In describing the behavior of ensembles of mesodefects of different structural levels, including microcracks and microshears, it is necessary to determine the form of microscopic and macroscopic parameters that take into account local changes in symmetry due to the presence of mesodefects and also the form of the dependence of the thermodynamic potential on structural variables characterizing the defects.

2.2. Microscopic and Macroscopic Variables for an Ensemble of Mesodefects. The structural variables associated with mesodefects were introduced in [7] as analogs of dislocation density tensors. These defects are described by symmetric tensors of the form

$$s_{ik} = s\nu_i\nu_k$$

in the case of microcracks and

$$s_{ik} = s(\nu_i l_k + l_i\nu_k)/2$$

in the case of microshears. Here $\boldsymbol{\nu} = (\nu_i, \nu_k)$ is the unit vector of the normal to the microcrack base or shear area, $\boldsymbol{l} = (l_i, l_k)$ is the unit vector in the shear direction, and s is the microcrack volume or shear intensity.

By averaging the microscopic tensor s_{ik}, we obtain the macroscopic tensor of density of mesodefects

$$p_{ik} = n\langle s_{ik}\rangle,$$

which has the meaning of strain due to defects; n is the concentration of defects.

2.3. Nonequilibrium Mesoscopic Potential of a Solid with Mesodefects. The study of the size distribution of mesodefects in strained solids shows that the spatial distribution of these defects at different scale levels possesses the properties of statistical self-similarity [7]. A consequence of this statistical self-similarity is a universal form of the distribution function of defects at different structural levels in some dimensionless (self-similar) coordinates. This property of an ensemble of mesodefects allowed a solution of a statistical problem of the behavior of an ensemble of defects to be proposed and the form of the nonequilibrium mesoscopic potential to be established in terms of intensive variables: tensor of density of defects p_{ik} and parameter of structural scaling δ [10, 11]. The parameter of structural scaling determined within the framework of the statistical description takes into account the role of structural scales in the case of a medium with defects. This parameter is the ratio of the mean distance between the defects L_H (close to the scale of the characteristic structural heterogeneity, for instance, to the grain size) to the mean size of defect nuclei L_N, for instance, the initial grain-boundary defects: $\delta = (L_H/L_N)^3$. The phenomenological presentation of the mesoscopic potential, which takes into account the known types of nonlinearity for a medium with mesodefects, has the form of the generalized Ginzburg–Landau expansion [12]

$$F = A(\delta, \delta_*)p_{ik}^2/2 - Bp_{ik}^4/4 + C(\delta, \delta_c)p_{ik}^6/6 - D\sigma_{ik}p_{ik} + \chi(\nabla p_{ik})^2, \tag{1}$$

where A, B, C, D, and χ are parameters of the medium, δ_* and δ_c are the critical values of the structural scaling parameter (points of bifurcation of the solution of the statistical problem), which are similar to the critical temperatures in Landau's theory of phase transitions and determine the types of the structural scaling transitions in a nonequilibrium mesoscopic system for different ranges of the values of the structural scaling parameter δ ($\delta > \delta_* \approx 1.3$, $\delta_c < \delta < \delta_*$, and $\delta < \delta_c \approx 1$).

3. PLASTICITY AND RELAXATION MECHANISMS AS STRUCTURAL SCALING TRANSITIONS IN MESODEFECT ENSEMBLES

The physical specific feature of the mechanism of momentum transfer under plastic strain implies that the dislocation carriers of plastic strain (in the present case, microshears) move in the field of conservative (elastic) forces. This is the main difference between irreversible deformation caused by reconstruction of the dislocation structure and reversible deformation.

Significant progress has been achieved in the last decades in studying plastic flow mechanisms and in developing the phenomenological theory of plasticity in a wide range of stresses and strain rates. At the moment, however, the use of structural characteristics in formulating the constitutive equations of plasticity does not offer any explanation for some specific features of plasticity mechanisms caused by dynamics of defects. The mechanisms of plastic strain localization (instability of localized shear), the relationship between the evolution of the structure and strain-induced hardening, and the universal character (self-similarity) of the plastic wave front have not be explained.

Experimental data on transitions in dislocation substructures under plastic strain and results of the statistical description of the collective behavior of microshear ensembles allow the relationship between plasticity and structural evolution to be established.

It was shown [13] that plastic deformation of a material can be considered as a consequence of structural accommodation of fragmented volumes of the material, which appear owing to ordering of dislocation ensembles in structural scaling transitions. Thus, plastic strain (in contrast to elastic strain) is not a thermodynamic variable of state; it is considered as a variable of the deformation process and is determined by dissipative mechanisms of the flow and structural changes in the material. Hence, we need to distinguish the contribution to entropy caused, on one hand, by dissipative processes (dissipative contribution) in the material flow and, on the other hand, by structural changes in the material due to formation of dislocation substructures of different scale levels.

To take into account the effect of structural relaxation on plastic flow during nonisothermal deformation, we determine the total strain rate from the kinematic relation

$$e_{ik} = \dot{\varepsilon}^p_{ik} + \dot{\varepsilon}^e_{ik} + \dot{p}_{ik} + e^T \delta_{ik}.$$

Here $\dot{\varepsilon}^p_{ik}$ is the plastic strain rate, $\dot{\varepsilon}^e_{ik}$ is the elastic strain rate, $\dot{p}_{ik}$ is the kinematic contribution of defects to the strain rate, and $e^T\delta_{ik}$ is the strain rate due to the thermoelastic effect.

Introducing into consideration the total free energy of the system $\Psi = W + F$ in the form of the sum of the free energies determined by elasticity (in particular, by thermoelasticity) of the medium (W) and by the contribution of mesodefects (F) and assuming that the free energy of the system depends only on the variables ε^e_{ik}, p_{ik}, and T, we can present the dissipative function of the system in the form

$$TP_s = \sigma_{ik} e^p_{ik} + \sigma_{ik}\dot{p}_{ik} - \frac{\partial F}{\partial p_{ik}}\,\dot{p}_{ik} \geqslant 0,$$

where the variables have a trace-free structure under the assumption of plastic incompressibility. In this case, the law of conservation of energy takes the form

$$c\rho\dot{T} = Q^e + Q^p + r - \nabla \boldsymbol{q},$$

where Q^e is the dissipative contribution due to thermoelasticity

$$Q^e = T\,\frac{\partial}{\partial \varepsilon^e_{ik}}\,\frac{\partial F}{\partial T} : e^e_{ik},$$

Q^p is the intensity of the source under plastic strain:

$$Q^p = T\,\frac{\partial}{\partial p_{ik}}\,\frac{\partial F}{\partial T} : \dot{p}_{ik} + \sigma_{ik} : e^p_{ik} + \Big(\sigma_{ik} - \frac{\partial F}{\partial p_{ik}}\Big) : \dot{p}_{ik}.$$

Under condition of a fixed sign of the dissipative function with allowance for the Onsager relations, the fluxes and thermodynamic forces are related as [13]

$$\sigma_{ik} = L^{(1)}_{iklm} e^p_{ik} - L^{(2)}_{iklm}\dot{p}_{ik}, \qquad \frac{\partial F}{\partial p_{ik}} = L^{(2)}_{iklm} e^p_{ik} - L^{(3)}_{iklm}\dot{p}_{ik}. \tag{2}$$

Equations (2) are quasi-linear: the kinetic coefficients $L^{(\nu)}_{iklm}$ depend in the general case on the invariants p_{ik}. These relations describe the "cross" effects: the influence of the kinetics of the dislocation subsystem on relaxation processes caused by the plastic flow of the medium.

4. DETERMINATION OF MODEL CONSTANTS

Based on the constitutive equations derived above, deformation of a solid under uniaxial loading with allowance for changes in temperature can be described by the following system of equations:

$$\rho\,\frac{\partial \dot{\varepsilon}}{\partial t} = \frac{\partial^2 \sigma}{\partial x^2}, \qquad \dot{\sigma} = E(e - \dot{\varepsilon}^p - \dot{p}),$$

$$\dot{\varepsilon}^p = l_1\sigma + l_2\Big(\sigma - \frac{\partial F}{\partial p}\Big), \qquad \dot{p} = l_3\Big(\sigma - \frac{\partial F}{\partial p}\Big) + l_2\sigma, \tag{3}$$

$$c\rho\dot{T}(x,t) = Q^e + \sigma(\dot{\varepsilon}^p + \dot{p}) - \frac{\partial F}{\partial p}\,\dot{p} + k\,\frac{\partial^2 T(x,t)}{\partial x^2}.$$

Here ε and σ are the components of the strain and stress tensors corresponding to the uniaxial case [$\varepsilon = (\nabla u + \nabla u^{\mathrm{t}})/2$ and σ is the Cauchy stress tensor], ε^p is the component of the plastic strain tensor, p is the component of the defect density tensor, F is the specific free energy due to the emergence of defects, $Q^e = TF_{T\varepsilon^e} : \dot{\varepsilon}^e$ is the heating due to the thermoelastic effect, ε^e is the component of the elastic strain tensor, and l_α are the first terms of expansion of the kinetic coefficients $L^{(\alpha)}_{iklm}$ with respect to the defect density tensor.

Let us estimate the characteristic times in Eq. (3). The system behavior is determined by heat transfer, localization of plastic strains, and momentum transfer. All three processes have significantly different characteristic

times: the characteristic time of propagation of elastic disturbances is $\tau_a \sim L/\sqrt{E/\rho} \sim 10^{-5}$ sec (L is the linear scale of the problem), the characteristic time of heat propagation is $\tau \sim L^2 c\rho/\lambda \sim 10^4$ sec (λ is the thermal conductivity), and the characteristic time of propagation of waves of structural relaxation and associated heat waves is $\tau_h \sim L/V_s \sim 10^2$ sec.

Assuming in Eq. (4) that $l_1 \gg l_2$, which physically corresponds to "subjection" of the plastic flow kinetics to structural relaxation and ignoring the influence of "cross" effects, we can write the constitutive equation for the plastic strain rate as $\dot{\varepsilon}^p = l_1\sigma$, which corresponds to the approximation of the Maxwellian medium in the description of relaxation properties. The expansion of the free energy in powers of the order parameter presents an adequate description of the system behavior near the phase transition. For obtaining numerical results in the entire range of stresses, however, expansion (1) in the numerical implementation was written in the form $\partial F/\partial p = (\partial F/\partial p)w(p)$, where $w(p)$ is a "window" function equal to zero in the elastic region and tending to unity in the transition region.

Thus, to describe the propagation of the heat wave and to determine its velocity, we analyzed the solution of the following system of equations:

$$\dot{p} = l_3\Big(\sigma - \frac{\partial F}{\partial p}\Big) + l_2\sigma, \qquad \frac{\partial F}{\partial p} = w(p)\Big(A_1 p + A_2 p^2 + A_3 p^3 - \frac{\partial}{\partial z}\,\chi(p)\,\frac{\partial p}{\partial z}\Big). \tag{4}$$

In the region of metastability, two equilibrium positions separated by a potential barrier correspond to each value of stress. Near the critical point, the right side of Eq. (3) can be presented as

$$\frac{\partial F}{\partial p} = \alpha(p - p_1)(p - p_2)(p - p_3) - \chi_0\,\frac{\partial^2}{\partial z^2}\,p,$$

where p_1, p_2, and p_3 are the solutions of the equation $\sigma - \partial F/\partial p = 0$; $\alpha \sim 10^2$ Pa.

Using new variables $\tau = l_3\chi_0 t$ and $p' = p - p_1$ (in what follows, the prime at p is omitted), we can write Eq. (4) in the form

$$\frac{\partial p}{\partial \tau} = \frac{\partial^2 p}{\partial z^2} - \frac{\alpha}{\chi_0}\,p(p_* - p)(p_c - p). \tag{5}$$

Equation (5) has the following analytical solutions [14] known as phase triggering waves:

$$p(\zeta) = p_*\,\frac{(C + p_c) + (C - p_c)\tanh\,(\zeta L_1^{-1})}{(C + p_*) + (C - p_*)\tanh\,(\zeta L_1^{-1})}, \qquad L_1 = \frac{\sqrt{8\chi_0/\alpha}}{p_* - p_c},$$

$$p(\zeta) = \frac{p_*}{1 + C\exp\,(\zeta L_2^{-1})}, \qquad L_2 = \frac{\sqrt{2\chi_0/\alpha}}{p_*}$$

($\zeta = x \pm V\tau$ and C is an arbitrary constant).

The expressions for wave-propagation velocities can be written as

$$V_1 = (p_* + p_c)\sqrt{\alpha}/\sqrt{2\chi_0}, \qquad V_2 = (p_* - 2p_c)\sqrt{\alpha}/\sqrt{2\chi_0}.$$

In terms of the initial variables, the velocity and width of the wave front (in the linear approximation) can be estimated as

$$L_2 = \sqrt{2\chi_0/\alpha}/(p_3 - p_1), \qquad V_2 = l_3\sqrt{\chi_0\alpha}\,(p_3 - 2p_2 + p_1)/\sqrt{2}$$

(p_1 and p_3 are the strains before and after wave transition, χ_0 is the non-locality parameter, and l_3 is the kinetic coefficient).

The experimental data plotted in Fig. 4 allow us to estimate the magnitude of the jump ($p_3 - p_1 \sim 5 \cdot 10^{-2}$) and the width of the wave front ($d = 2 \cdot 10^{-2}$ m). The front width can be estimated on the basis of structural changes or on the basis of the estimate of the characteristic size of moving heat sources. In this case, we obtain the non-locality parameter $\chi_0 = \alpha(L_2(p_3 - p_1))^2/2 \approx 10^2 \cdot (10^{-3})^2/2 = 5 \cdot 10^{-5}$ m$^2\cdot$Pa and the kinetic coefficient $l_3 = \sqrt{2}\,V_1(\alpha\chi_0)^{-1/2}/(p_3 + p_2 - 2p_1) \approx \sqrt{2} \cdot 10^{-4} \cdot (10^2 \cdot 5 \cdot 10^{-5})^{-1} \cdot 10^2 \approx 0.2$ sec^{-1}; hence, the relaxation time is estimated as $\tau \sim (l_3\alpha p_3 p_1)^{-1} \approx 10^{-5}$ sec.

For verification of the model, we studied the regime of uniaxial deformation of the sample in the x direction. The following values of physical quantities were used in the calculations: density $\rho = 7870$ kg/m^3, heat capacity $c = 420$ J/(kg$\cdot\,^\circ$C), Young's modulus $E = 2 \cdot 10^{11}$ Pa, and thermal conductivity $\lambda = 40$ W/(m$\cdot\,^\circ$C).

The function $\chi(p)$ can be presented in the form

$$\chi(p) = \chi_0 + \chi_1 p + \chi_2 p^2 + \chi_3 p^3 + \dots\ . \tag{6}$$

In modeling the propagation of heat waves, we left only the first term in expansion (6).

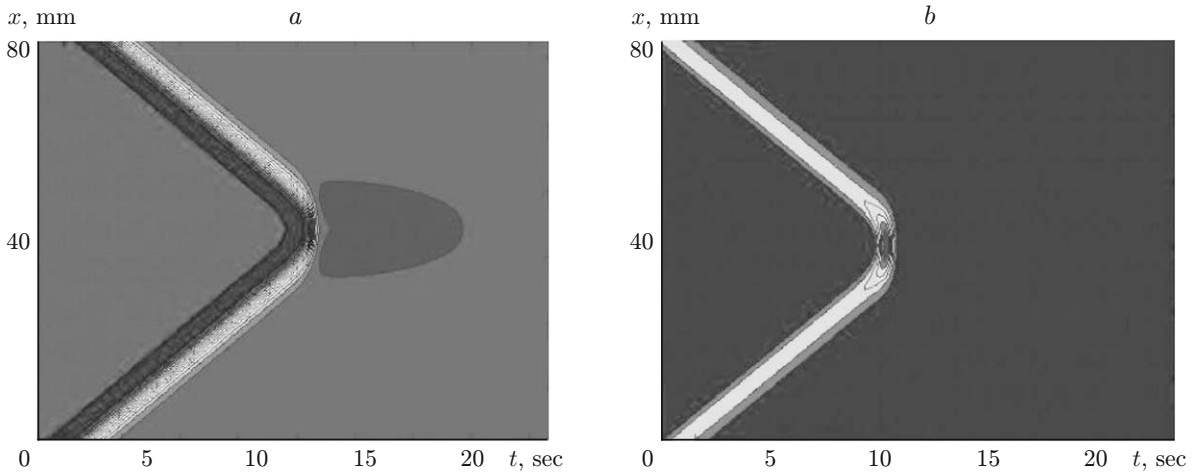

Fig. 5. Space–time evolution of the temperature field (a) and the corresponding distribution of heat sources (b) obtained in calculations.

5. RESULTS OF NUMERICAL CALCULATIONS AND COMPARISON WITH EXPERIMENTAL DATA

The system of equations was solved numerically. The sample length was chosen to be 0.1 m, and the strain rate was $2 \cdot 10^{-3}$ sec^{-1}. The influence of the clutches on the evolution of the stress field in the sample was modeled by a finite-amplitude perturbation of the field of structural deformation on the sample boundary $p(0, t)$. Depending on the value of the structural scaling parameter, structural transitions of different types can occur in an ensemble of defects. In the range $\delta_c < \delta < \delta_*$, the system has defects with two equilibrium concentrations divided by a potential barrier ΔF. The value of the barrier depends on the current value of stress and decreases with penetration into the metastability region. At a certain time, the fluctuations of the boundary conditions become commensurable with the magnitude of the potential barrier, and the system transforms from one equilibrium state to the other in a jumplike manner on the sample boundaries, which involve initiation of a triggering wave.

Figure 5 shows the space–time distribution of the temperature field and the corresponding distribution of the field of heat sources. As is seen from experimental results, wave propagation leads to localization of the deformation process. Figure 4 shows the calculated and experimental curves of the local strain evolution.

Results of numerical calculations are in good qualitative agreement with experimental data. To quantify these results, we have to solve a coupled problem with allowance for acoustic, structural, and thermal processes. In particular, the condition $\sigma = \text{const}$ imposed in solving the problem is equivalent to the condition of equality of the total rate of structural deformation and strain rate in the sample: $\int_0^L \dot{p}\, dx = v^g L$ (v^g is the velocity of motion of the clutches). In the case with $\int_0^L \dot{p}\, dx > v^g L$, the boundary conditions prevent reaching the equilibrium state at all points behind the wave front; for this reason, the waves can propagate twice over the same part of the sample. Figure 6 shows the experimentally observed pattern of propagation of heat sources for a strain rate $\dot{\varepsilon} = 10^{-3}$ sec^{-1}. After their meeting, the waves continue to propagate over the sample surface for some time; as a result, the structural transition becomes completed.

CONCLUSIONS

Based on an experimental and theoretical study of the processes of propagation of strain localization waves, a model for energy dissipation and plastic flow in metals is proposed; the model takes into account the specific

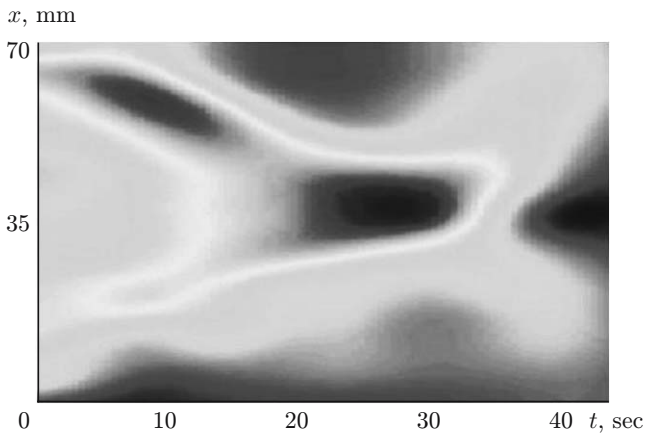

Fig. 6. Space–time distribution of heat sources on the sample surface for a strain rate $\dot{\varepsilon} = 10^{-3}$ sec^{-1}.

features of the evolution of an ensemble of mesodefects (microshears). Based on a statistical description of an ensemble of mesodefects, the characteristic responses of the material to the growth of defects are determined, and the constitutive equations that describe the total energy balance in a deformed solid are derived.

A specific feature of the approach developed is the presentation of plastic strain as the sum of two variables: plastic strain ε_{ik}^{p} related to the kinetics of defects and structural strain p_{ik}. This presentation allows the "structural" component of the plastic strain to be considered as an independent thermodynamic variable; hence, the form of the corresponding thermodynamic potential can be determined.

An analysis of the constitutive equations obtained showed that plastic strain localization can move over the sample surface and initiate a heat wave; the evolution of plastic strain is similar to the evolution of the wave of phase transformation and can be described in terms used in the Ginzburg–Landau approach. The amplitude of the strain localization wave is determined by the difference in the values of structural deformation at the points on the thermodynamic curve corresponding to the given stress. It should be noted that the length of the plateau corresponding to plastic strain is determined in this model both by the properties of the material sample and by its geometric sizes.

The authors are grateful to the team of the LAMEFIP-ENSAM laboratory for their assistance in experiments and also to N. Saintier and T. Palin-Luc for useful discussions.

This work was supported by the Russian Foundation for Basic Research (Grant Nos. 07-08-96001 and 07-01-91100).

REFERENCES

1. V. E. Panin (ed.), *Physical Mesomechanics and Computer-Aided Design of Materials* [in Russian], Nauka, Moscow (1995).
2. H. Louche and A. Chrysochoos, "Thermal and dissipative effects accompanying Luders band propagation," *Mater. Sci. Eng.*, **A307**, 15–22 (2001).
3. V. I. Danilov, S. A. Barannikova, and L. B. Zuev, "Self-sustained waves of localized plastic deformation at the initial stages of plastic flow of single crystals," *Zh. Tekh. Fiz.*, **73**, No. 11, 69–75 (2003).
4. S. P. Kiselev, "Dislocation structure of shear bands in single crystals," *J. Appl. Mech. Tech. Phys.*, **47**, No. 6, 857–866 (2006).
5. W. S. Farren and G. I. Taylor, "The heat developed during plastic extension of metals," *Proc. Roy. Soc. London*, **A107**, 422–451 (1925).
6. O. B. Naimark and O. V. Ladygin, "Nonequilibrium kinetic transitions in solids as mechanisms of local plastic strain localization," *J. Appl. Mech. Tech. Phys.*, **34**, No. 3, 427–432 (1993).
7. O. B. Naimark, "Collective properties of ensembles of defects and some nonlinear problems of plasticity and fracture," *Fiz. Mezomekh.*, **6**, No. 4, 45–72 (2003).

8. A. Chrysochoos and H. Louche, "An infrared image processing to analyse the calorific effects accompanying strain localization," *Int. J. Eng. Sci.*, **38**, 1759–1788 (2000).
9. J. Gilman, "Mechanical states of solids," in: *Shock Compression of Condensed Materials*, Proc. of the 12th APS Conf. (Atlanta, June 24–29, 2001), Amer. Inst. of Phys., New York (2002), pp. 36–41.
10. O. B. Naimark, M. M. Davydova, O. A. Plekhov, and S. V. Uvarov, "Experimental and theoretical study of the dynamic stochasticity and scaling for crack propagation," *Fiz. Mezomekh.*, **2**, No. 3, 47–58 (1999).
11. O. B. Naimark, "Defect induced transitions as mechanisms of plasticity and failure in multifield continua," in: *Advances in Multifield Theories of Continua with Substructure*, Birkhauser, Boston (2003), pp. 75–114.
12. O. B. Naimark, "Void formation, equations of state, and stability of superplastic deformation of materials," *J. Appl. Mech. Tech. Phys.*, **26**, No. 4, 585–591 (1985).
13. V. V. Belyaev and O. B. Naimark, "Kinetic transitions in media with microcracks and metal fracture in stress waves," *J. Appl. Mech. Tech. Phys.*, **28**, No. 1, 157–164 (1987).
14. A. D. Polyanin and V. F. Zaitsev, *Nonlinear Equations of Mathematical physics: Exact Solutions* [in Russian], Fizmatlit, Moscow (2002).